JOC The Journal of Organic Chemistry

Article

pubs.acs.org/joc

Chemical Bonding and Aromaticity in Furan, Pyrrole, and Thiophene: A Magnetic Shielding Study

Kate E. Horner and Peter B. Karadakov*

Department of Chemistry, University of York, Heslington, York YO10 5DD, U.K.

ABSTRACT: Aromaticity and bonding in furan, pyrrole, and thiophene are investigated through the behavior of the isotropic shielding $\sigma_{iso}(\mathbf{r})$ within the regions of space surrounding these molecules. HF-GIAO/6-311++G(d,p) and MP2-GIAO/6-311++G(d,p) (Hartree–Fock and second-order Møller–Plesset perturbation theory utilizing gauge-including atomic orbitals) $\sigma_{iso}(\mathbf{r})$ contour plots are constructed using regular two-dimensional 0.05 Å grids in the molecular plane, in horizontal planes 0.5 and 1 Å above it, and in a vertical plane through the heteroatom. The nucleus-independent chemical shifts (NICS) calculated at the ring centers and at 0.5 Å and 1 Å above these centers, NICS(0), NICS(0.5), and NICS(1), respectively, support the widely accepted order of aromaticities thiophene > pyrrole > furan. The results suggest that accurate NICS calculations benefit more from the use of an extended basis set than from the inclusion of dynamical electron correlation effects. The different extents of $\sigma_{iso}(\mathbf{r})$ delocalization observed in the horizontal contour plots and other features of $\sigma_{iso}(\mathbf{r})$ are also consistent with an aromaticity reduction of the order thiophene > pyrrole > furan. It is suggested that the extent of $\sigma_{iso}(\mathbf{r})$ delocalization in $\sigma_{iso}(\mathbf{r})$ contour plots in planes 1 Å above the molecular plane could be used for comparing the relative aromaticities of a wide range of aromatic systems.

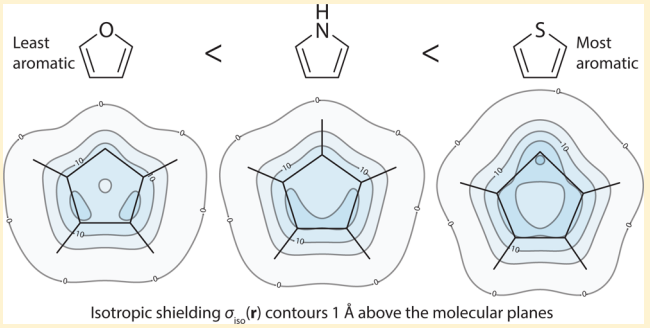

1. INTRODUCTION

The magnetic shielding tensor is an important source of information about the electronic environment of any point within the space surrounding a molecular system. This second-rank tensor was introduced in nuclear magnetic resonance (NMR) theory where it is used to explain the observation that chemically inequivalent nuclei exhibit different degrees of shielding. The elements of the magnetic shielding tensor of nucleus J can be calculated as second-order response properties using the expression

$$\sigma_{J,\alpha\beta} = \left.\frac{\partial^2 E(\{\mathbf{m}_I\}, \mathbf{B})}{\partial \mathbf{m}_{J,\alpha} \partial \mathbf{B}_\beta}\right|_{\forall \mathbf{m}_I = 0, \mathbf{B} = 0} \quad (1)$$

where $E(\{\mathbf{m}_I\},\mathbf{B})$ is the energy of a molecular system with nuclear magnetic moments $\{\mathbf{m}_I\}$ in the presence of a uniform magnetic field $\mathbf{B}$. The isotropic shielding of nucleus J is defined as

$$\sigma_{J,\mathrm{iso}} = \frac{1}{3}(\sigma_{J,xx} + \sigma_{J,yy} + \sigma_{J,zz}) \quad (2)$$

The magnetic shielding tensor and the isotropic shielding can be evaluated not just at nuclear positions, but also at any point $\mathbf{r}$ within the space surrounding the molecule, at which there is some non-negligible electronic density, as $\boldsymbol{\sigma}(\mathbf{r})$ and $\sigma_{iso}(\mathbf{r})$, respectively.

Since the 1958 paper by Johnson and Bovey,[1] there has been growing interest in evaluating magnetic shielding tensor-related properties at off-nucleus positions. Johnson and Bovey used Pauling's free electron model to calculate the magnetic field around a benzene molecule and, consequently, the shifts in the NMR shielding values which would be experienced by protons placed at different points within a plane passing normally through the center of the ring. This approach provided interesting insights into ring current effects, which have traditionally been considered responsible for the experimentally observed noticeable deshielding of arene protons, although it has also been argued that this deshielding is not due to ring currents.[2]

More recently, molecular probes placed at selected positions within the space surrounding a molecular system have been used by Martin et al.[3−5] to analyze through-space NMR shielding effects and to look for signs of aromatic, or the antithetical antiaromatic, behavior. As is well known, it is very difficult to formulate unambiguous and universal quantitative measurements of the elusive concepts of aromaticity and antiaromaticity. One drawback associated with the use of a molecular probe is that it perturbs the wave function of the molecule under investigation (see e.g., ref 6) and renders any property calculated with this wave function dependent on the nature of the probe. The effects associated with the presence of a spectator atom or molecule are eliminated in the nucleus-independent chemical shift (NICS) technique developed by Schleyer and et al.[7] The original NICS approach, currently

Received: June 18, 2013
Published: July 23, 2013

   dx.doi.org/10.1021/jo401319k | J. Org. Chem. 2013, 78, 8037−8043

Table 1. Isotropic Shieldings for the Symmetry-Unique Nuclei and NICS(0), NICS(0.5), and NICS(1) Values (in ppm) for Furan, Pyrrole, and Thiophene Calculated at the HF-GIAO/6-311++G(d,p) and MP2-GIAO/6-311++G(d,p) Levels of Theory[a]

	furan (Z=O)		pyrrole (Z=N)		thiophene (Z=S)	
property	HF-GIAO	MP2-GIAO	HF-GIAO	MP2-GIAO	HF-GIAO	MP2-GIAO
$\sigma_{iso}(Z)$	57.70	56.29	109.10	117.76	333.73	314.05
$\sigma_{iso}(H_Z)$			24.85	24.19		
$\sigma_{iso}(C_1)$	41.80	54.55	68.16	83.13	55.47	73.61
$\sigma_{iso}(C_2)$	78.88	89.39	79.48	89.18	62.74	73.97
$\sigma_{iso}(H_1)$	24.49	24.31	25.15	25.12	24.66	24.59
$\sigma_{iso}(H_2)$	25.64	25.41	25.67	25.41	24.92	24.62
NICS(0)	−12.18	−12.64	−14.80	−14.14	−19.64	−19.43
NICS(0.5)	−11.57	−12.11	−13.53	−13.07	−16.56	−16.62
NICS(1)	−9.20	−9.70	−10.42	−10.25	−11.35	−11.68

[a] C_1 is the carbon adjacent to the heteroatom Z.

referred to as NICS(0), evaluates the isotropic shielding at the ring center of an (anti)aromatic system which is then taken with a reversed sign, $-\sigma_{iso}$. Over the years, NICS(0) and other NICS indices, such as dissected NICS, NICS(1), etc., have become some of the most popular aromaticity probes. In dissected NICS,[8,9] the σ and π components of NICS are separated. In NICS(1),[9,10] the NICS is evaluated 1 Å above the ring center with the aim to focus on the ring current effects associated with π electrons by reducing the σ electron contributions.

Various aspects of the NICS approach have been subject to criticism, for example, the fact that NICS are not experimentally measurable.[11] Research on ring currents carried out by Bultinck et al.[12] suggests that reduction of a global molecular property such as the current density map to a single NICS value could lead to significant loss of information and make it difficult to distinguish between systems which have similar NICS values but exhibit quite different ring currents. In this context, intuition suggests that it would be appropriate to study not just NICS calculated at selected points in space but also the overall behavior of the off-nucleus isotropic shielding, at a similar level of detail as current density maps. This idea was explored in 2001 by Klod and Kleinpeter[13] who decided to evaluate the isotropic shieldings $\sigma_{iso}(\mathbf{r})$ for the molecule under investigation at a regular grid of points spaced 0.5 Å apart between −10 and 10 Å along each coordinate axis and used the results to construct isotropic chemical shielding surfaces (ICSSs). These authors demonstrated that the ICSSs could be used to investigate the anisotropy effects of various functional groups, ring currents, and the influence of heteroatoms. ICSSs were applied to a range of aromatic and antiaromatic systems in reference 14.

We have shown[15] that working with a finer grid of points with a spacing of 0.05 Å in each direction allows the construction of much more detailed $\sigma_{iso}(\mathbf{r})$ isosurfaces and contour plots which can be used not only to distinguish between aromatic and antiaromatic systems, such as benzene and cyclobutadiene, but also to characterize chemical bonds and investigate the extents to which these bonds are affected by the aromatic or antiaromatic nature of the molecule in which they reside.

The aims of this paper are to examine in detail the variations in the isotropic shielding $\sigma_{iso}(\mathbf{r})$ within the space surrounding the aromatic five-membered heterocycles with one heteroatom furan, pyrrole, and thiophene and to use the results to highlight the differences in aromaticity and bonding in these molecules.

2. COMPUTATIONAL PROCEDURE

The isotropic magnetic shielding values reported in this paper were obtained using the Hartree−Fock (HF) method and second-order Møller−Plesset perturbation theory (MP2) with molecular orbitals expanded in terms of gauge-including atomic orbitals (GIAOs). All HF-GIAO and MP2-GIAO calculations were performed within the 6-311++G(d,p) basis at the experimental gas-phase ground-state equilibrium geometries of furan,[16] pyrrole,[17] and thiophene[18] by means of Gaussian 09.[19]

To study the variations of the isotropic shielding in the regions of space surrounding furan, pyrrole, and thiophene, $\sigma_{iso}(\mathbf{r})$ was evaluated in four planes for each molecule. For this, we used regular 7 Å × 7 Å two-dimensional grids of points with a spacing of 0.05 Å that were centered at or directly above the center of mass. The first plane was the molecular plane, the second and third planes were chosen to be parallel to the molecular plane and 0.5 or 1 Å above it, respectively, and the fourth plane was vertical, perpendicular to the molecular plane, and passing through the heteroatom and the midpoint of the opposite carbon−carbon bond. The computational effort was reduced by taking into account the C_{2v} symmetry exhibited by all three heterocycles. The number of symmetry-unique points in the grid for each plane was thus reduced from 141^2 to 71 × 141.

The grid points are specified in a Gaussian 09 input file as ghost atoms without basis functions (symbol Bq). The Gaussian 09 input routines limit the number of ghost atoms within a single geometry specification, which made it necessary to perform a number of separate NMR calculations including 95 ghost atoms each. The CPU time for an NMR calculation with 95 ghost atoms on furan, pyrrole, or thiophene was observed to be about three times longer than that for an analogous NMR calculation without ghost atoms. In order to ensure sufficient accuracy of the results, all calculations were carried out with the self-consistent field (SCF) "SCF(Tight)" convergence criterion (this is the Gaussian 09 default) and with the coupled perturbed Hartree−Frock (CPHF) "CPHF(Separate)" keyword.

3. RESULTS AND DISCUSSION

The isotropic shieldings for all symmetry-unique nuclei in furan, pyrrole, and thiophene, as well as the NICS(0), NICS(0.5) (NICS evaluated 0.5 Å above the ring center), and NICS(1) values for these heterocycles, obtained during the calculations of the respective grids of $\sigma_{iso}(\mathbf{r})$ data, are shown in Table 1.

As expected, the C_1 carbons which are connected to more electronegative heteroatoms are less shielded than the C_2 carbons. The differences between $\sigma_{iso}(C_1)$ and $\sigma_{iso}(C_2)$ decrease at the MP2-GIAO level of theory, and while the C_1 carbons in furan still remain considerably less shielded, by ca. 35 ppm, than the C_2 carbons, the $\sigma_{iso}(C_1)$ and $\sigma_{iso}(C_2)$ values in pyrrole and thiophene get much closer, to within ca. 6 ppm and

dx.doi.org/10.1021/jo401319k | J. Org. Chem. 2013, 78, 8037−8043

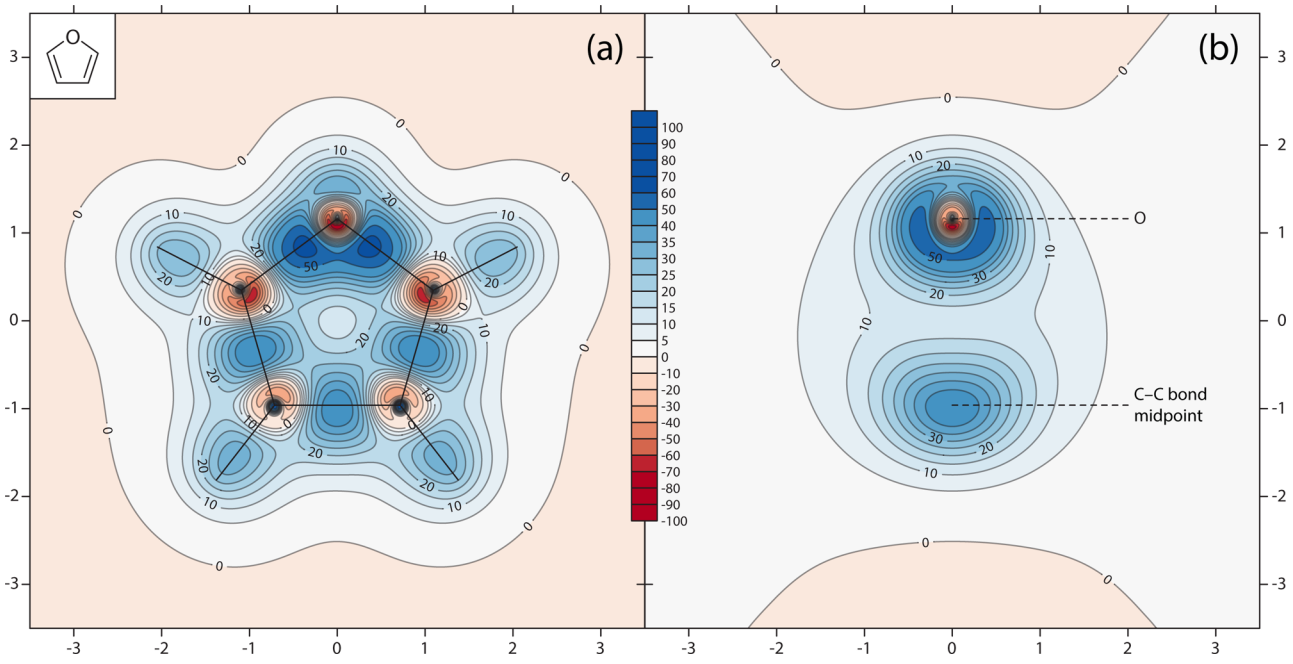

Figure 1. Contour plots of the isotropic shielding $\sigma_{iso}(\mathbf{r})$ (in ppm) for furan in (a) the molecular plane and (b) a vertical plane perpendicular to the molecular plane and passing through the oxygen atom and the midpoint of the opposite carbon−carbon bond.

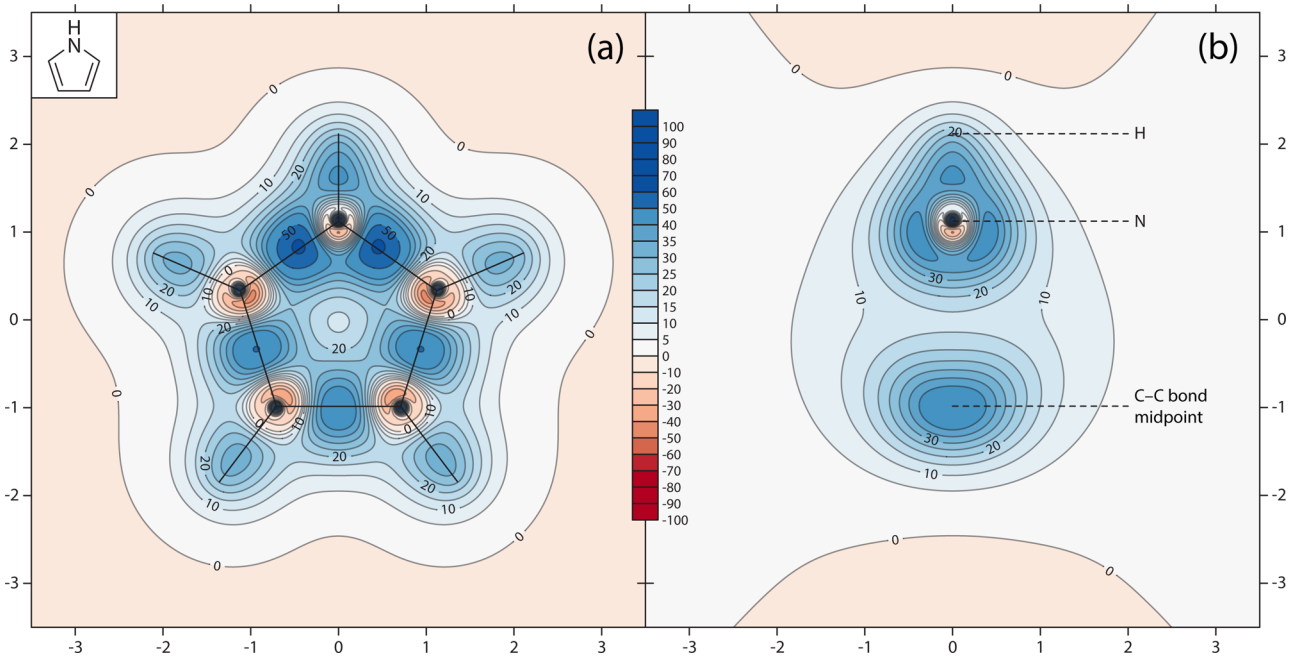

Figure 2. Contour plots of the isotropic shielding $\sigma_{iso}(\mathbf{r})$ (in ppm) for pyrrole in (a) the molecular plane and (b) a vertical plane perpendicular to the molecular plane and passing through the nitrogen atom and the midpoint of the opposite carbon−carbon bond.

ca. 0.4 ppm, respectively. Another interesting observation is that the MP2-GIAO isotropic shieldings for the O and C_1 nuclei in furan differ by less than 2 ppm. Apart from O in furan, the differences between the HF-GIAO and MP2-GIAO isotropic shieldings for the heavy nuclei are considerable, which suggests that the corresponding MP2-GIAO/6-311++G(d,p) values are likely to change by another 5−10 ppm at higher levels of theory. On the other hand, the differences between the HF-GIAO and MP2-GIAO proton shieldings and NICS values are much smaller, under 0.5 ppm. The same observation can be made about the off-nucleus isotropic chemical shieldings, $\sigma_{iso}(\mathbf{r})$: the plots of HF-GIAO and MP2-GIAO $\sigma_{iso}(\mathbf{r})$ values are almost visually indistinguishable; as a consequence, we present and discuss only the plots obtained at the higher level of theory.

All NICS(0), NICS(0.5), and NICS(1) values reported in Table 1 indicate that thiophene is more aromatic than pyrrole which, in turn, is more aromatic than furan. This is in contrast to the HF-GIAO/6-31+G* and HF-GIAO/6-31G* NICS(0) results of Schleyer et al.[7] according to which aromaticity should decrease in the order pyrrole > thiophene > furan.

dx.doi.org/10.1021/jo401319k | J. Org. Chem. 2013, 78, 8037−8043

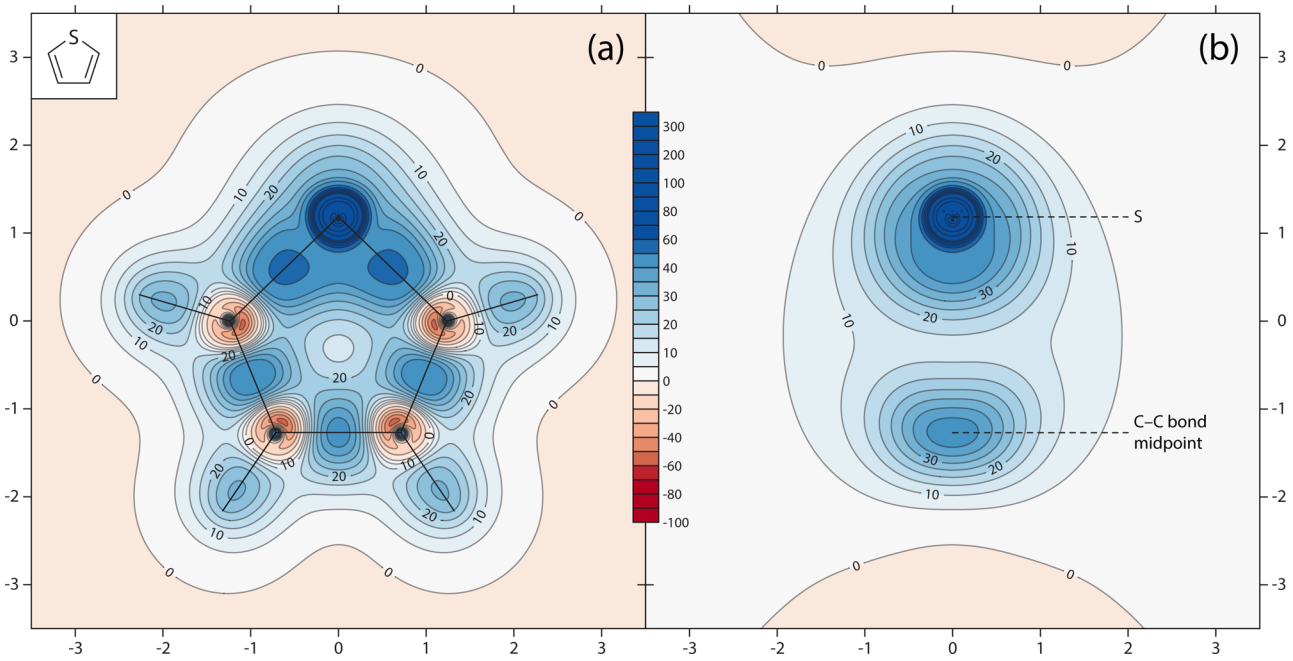

Figure 3. Contour plots of the isotropic shielding $\sigma_{iso}(\mathbf{r})$ (in ppm) for thiophene in (a) the molecular plane and (b) a vertical plane perpendicular to the molecular plane and passing through the sulfur atom and the midpoint of the opposite carbon−carbon bond.

The variations in the isotropic shielding $\sigma_{iso}(\mathbf{r})$ within the volumes of space surrounding furan, pyrrole, and thiophene are illustrated by the contour plots in Figures 1−6. The contour plots of $\sigma_{iso}(\mathbf{r})$ in the molecular planes of all three five-membered cycles (see Figures 1a, 2a, and 3a) show very clear pictures of the chemical bonding in these molecules, with carbon−heteroatom, carbon−carbon, carbon−hydrogen, and heteroatom−hydrogen bonds enclosed within regions of increased shielding. These contour plots support the widely accepted notion that the C_1-C_2 "double" bonds in furan, pyrrole, and thiophene are stronger than the $C_2'-C_2''$ "single" bonds, but they indicate that the differences are relatively small, which is also reinforced by the highest $\sigma_{iso}(\mathbf{r})$ values within bond regions reported in Table 2. There is less similarity between the regions above (and below) the C_1-C_2 and $C_2'-C_2''$ bonds shown in the contour plots of $\sigma_{iso}(\mathbf{r})$ in planes 0.5 and 1 Å above the molecular planes (see Figures 4−6), which suggests that the differences between these bonds are mainly in their π components.

Table 2. Highest Isotropic Shieldings within Regions Corresponding to Carbon−Heteroatom and Carbon−Carbon Bonds in Furan, Pyrrole, and Thiophene (in ppm)[a]

	highest $\sigma_{iso}(\mathbf{r})$ value		
bond	furan (Z=O)	pyrrole (Z=N)	thiophene (Z=S)
C_1-Z	64	61	54
C_1-C_2	47	50	49
$C_2'-C_2''$	45	48	44

[a]Approximate values taken from the $\sigma_{iso}(\mathbf{r})$ grids in the respective molecular planes calculated at the MP2-GIAO/6-311++G(d,p) level of theory.

The degree of aromaticity of an aromatic system is often associated with bond equalization.[20] We can use the contour plots shown in Figures 1a, 2a, 3a, and 4−6 as well as the data in Table 2 to compare the shielded regions along the carbon−carbon and carbon−heteroatom bonds in furan, pyrrole, and thiophene. The most pronounced "disruption" to bond equalization in these rings is associated with the introduction of the heteroatom. In this respect, equalization in the bonds involving the heteroatom can be considered to be more important than equalization between the remaining carbon−carbon bonds. Visually, the most "equalized" distribution of shielded regions corresponding to the bonds making up a ring is observed in thiophene, and then in pyrrole, followed by furan. The difference between the highest $\sigma_{iso}(\mathbf{r})$ values over carbon−heteroatom and carbon−carbon double bonds in thiophene is surprisingly small, ca. 5 ppm, against ca. 11 ppm in pyrrole and ca. 17 ppm in furan (see Table 2). The largest variation in the highest $\sigma_{iso}(\mathbf{r})$ values along all bonds making up the ring in thiophene is 10 ppm, compared to 13 ppm in pyrrole and 19 ppm in furan. These observations suggest that thiophene is slightly more aromatic than pyrrole, which, in turn, is more aromatic than furan.

A noteworthy feature of all contour plots in planes passing through at least one sp^2 hybridized atom is that the nuclei of such atoms are surrounded by deshielded regions within which $\sigma_{iso}(\mathbf{r})$ is negative. Very close to the nucleus of the sp^2 hybridized atom, $\sigma_{iso}(\mathbf{r})$ becomes positive again and then quickly increases up to the value calculated at the nucleus. Analogous deshielded regions around carbon nuclei have been reported to result from HF-GIAO, MP2-GIAO, and CASSCF-GIAO (complete-active-space self-consistent field approach utilizing GIAOs) $\sigma_{iso}(\mathbf{r})$ calculations on benzene and a CASSCF-GIAO $\sigma_{iso}(\mathbf{r})$ calculation on cyclobutadiene.[15] In all HF-GIAO, MP2-GIAO, and CASSCF-GIAO calculations of $\sigma_{iso}(\mathbf{r})$ isosurfaces in saturated and unsaturated hydrocarbons we have carried out so far, deshielded regions are observed to surround the nuclei of sp^2 and sp hybridized carbon atoms, but not those of sp^3 hybridized carbons. The current HF-GIAO and MP2-GIAO calculations of $\sigma_{iso}(\mathbf{r})$ in furan, pyrrole, and thiophene show deshielded "halos" not only around the carbons, but also around the oxygen in furan and the nitrogen

dx.doi.org/10.1021/jo401319k | J. Org. Chem. 2013, 78, 8037−8043

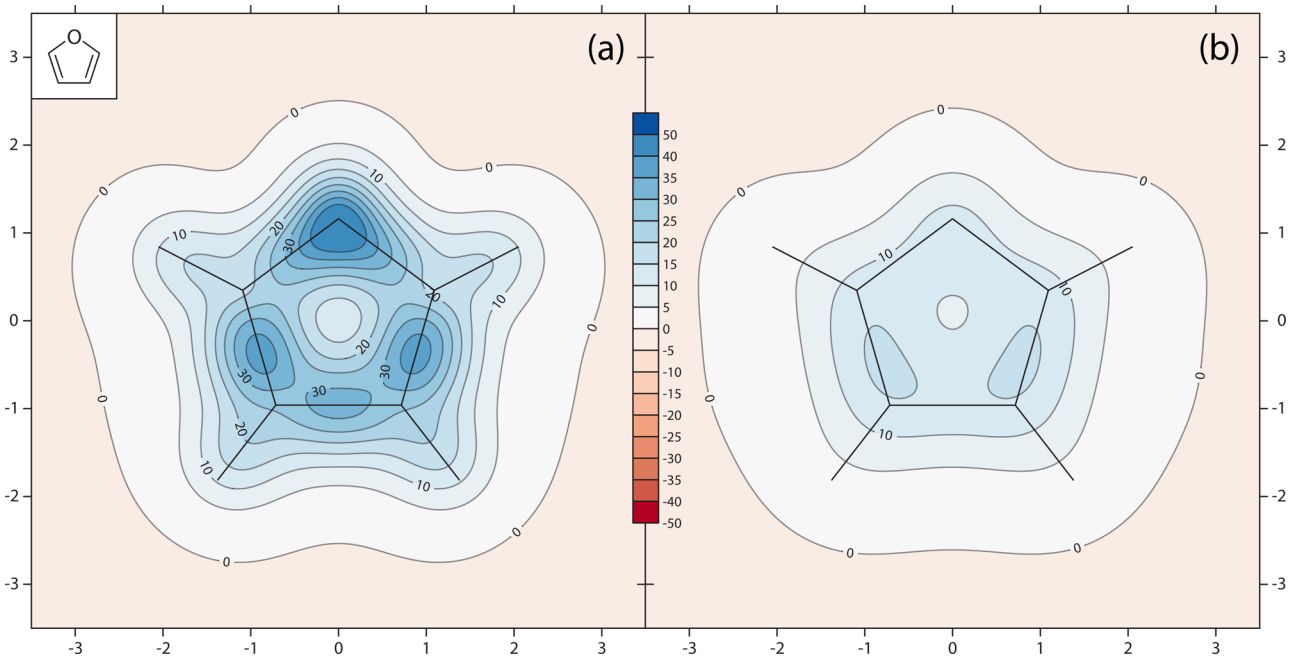

Figure 4. Contour plots of the isotropic shielding $\sigma_{iso}(\mathbf{r})$ (in ppm) for furan in planes (a) 0.5 Å and (b) 1 Å above the molecular plane.

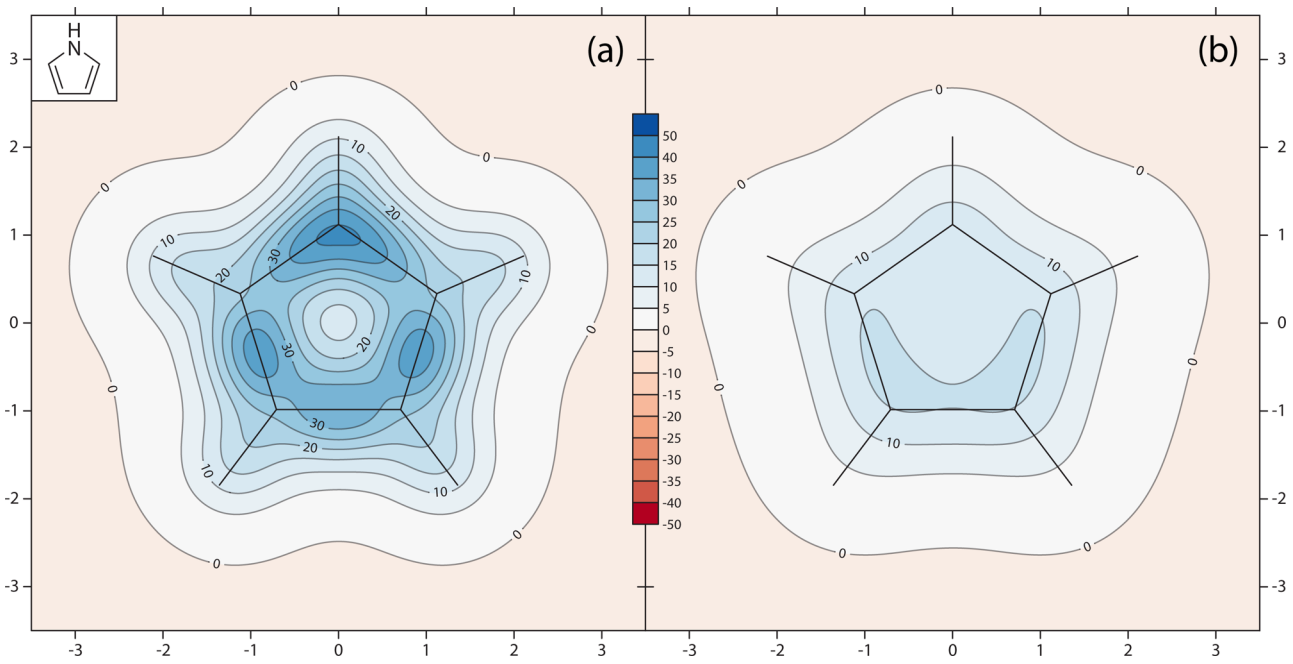

Figure 5. Contour plots of the isotropic shielding $\sigma_{iso}(\mathbf{r})$ (in ppm) for pyrrole in planes (a) 0.5 Å and (b) 1 Å above the molecular plane.

in pyrrole. However, there is no such halo around the sulfur in thiophene, a third-row atom. The explanation for the selective appearance of deshielded halos around the nuclei of sp^2 and sp hybridized second-row atoms is not straightforward and requires further research, either through a detailed analysis of ring currents or through the calculation of dissected $\sigma_{iso}(\mathbf{r})$ contour plots and isosurfaces, defined analogously to dissected NICS (see e.g., ref 22 and references therein).

A closer inspection of the deshielded regions around the carbon nuclei in furan, pyrrole, and thiophene reveals some interesting differences between the three molecules. In furan (see Figure 1a), the two C_1 carbon nuclei adjacent to the oxygen are encompassed within deshielded regions which are noticeably larger and less shielded than those around the C_2 carbon nuclei. As observed previously in $\sigma_{iso}(\mathbf{r})$ calculations on benzene and cyclobutadiene,[15] the minimum $\sigma_{iso}(\mathbf{r})$ value within each deshielded region is positioned within the frontal part of a lobe pointing toward the center of the ring. In pyrrole (see Figure 2a), the differences between the deshielded immediate neighborhoods of the C_1 and C_2 carbon nuclei are significantly less pronounced. Finally, in thiophene (see Figure 3a), the deshielded regions around the C_1 and C_2 carbon nuclei are almost identical and reasonably similar to those in benzene.[15] Thus, when following the series furan, pyrrole, thiophene, the differences between the isotropic shielding environments of the C_1 and C_2 carbon nuclei decrease, and

dx.doi.org/10.1021/jo401319k | J. Org. Chem. 2013, 78, 8037−8043

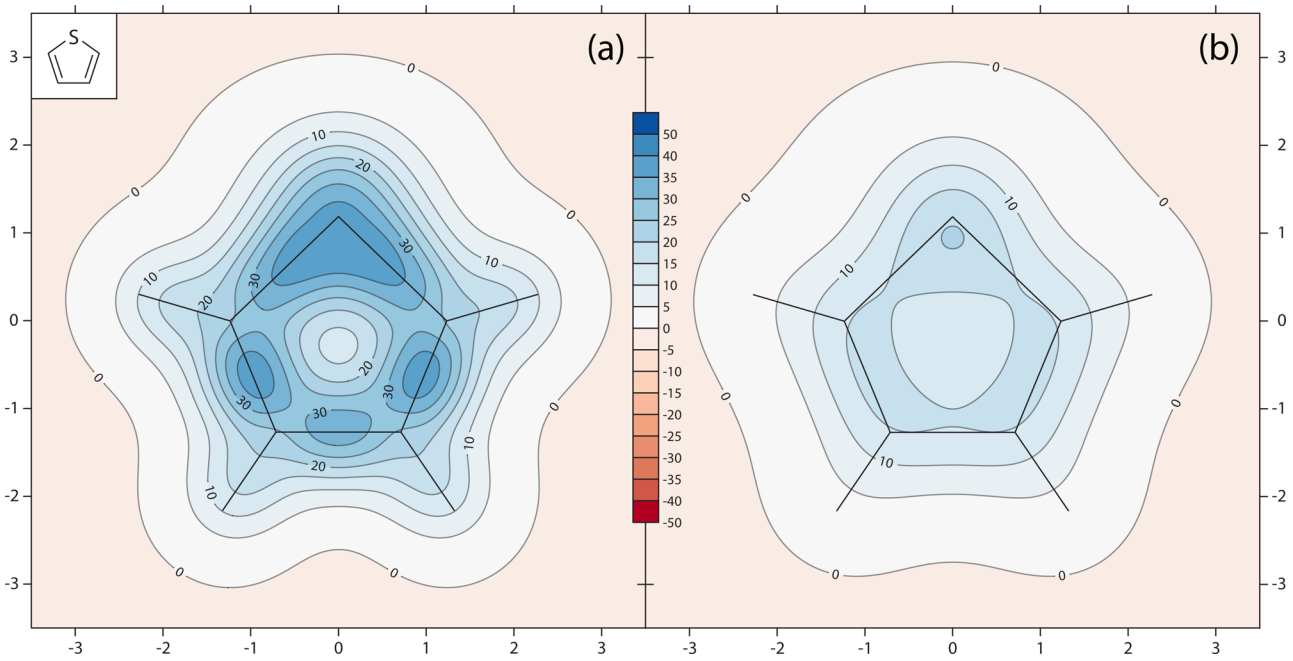

Figure 6. Contour plots of the isotropic shielding $\sigma_{iso}(\mathbf{r})$ (in ppm) for thiophene in planes (a) 0.5 Å and (b) 1 Å above the molecular plane.

these environments become closer in shape and composition to that in benzene. The deshielded regions around carbon nuclei in cyclobutadiene were reported to resemble in shape those of benzene, but they go down to significantly lower $\sigma_{iso}(\mathbf{r})$ values,[15] similar to the surroundings of the C_1 carbon nuclei in furan. These observations lend further support to the notion that the aromaticity of the three five-membered rings increases in the order furan < pyrrole < thiophene.

The contour plots of $\sigma_{iso}(\mathbf{r})$ in the vertical symmetry planes passing through the heteroatom and the opposite carbon−carbon bond (see Figures 1b, 2b, and 3b) provide further details about the shapes of the deshielded regions surrounding the oxygen and nitrogen nuclei in furan and pyrrole, respectively, and the shape of the shielded region about the sulfur nucleus in thiophene. The cross sections of the carbon−carbon bonds opposite heteroatoms shown in these figures have very similar shapes, but a keen observer can notice the switch from a more oval, in furan and pyrrole, to a slightly kidney-like shape in thiophene. The latter bears closer resemblance to the shapes of the cross sections of $\sigma_{iso}(\mathbf{r})$ through the midpoints of the carbon−carbon bonds in benzene.[15]

Overall, the $\sigma_{iso}(\mathbf{r})$ contour plots shown in Figures 1b, 2b, and 3b are not that different in appearance from the corresponding total electronic density contour plots for furan, pyrrole, and thiophene calculated by Cordell and Boggs at the HF level of theory.[23] Naturally, the deshielded regions surrounding the oxygen and nitrogen nuclei have no equivalents in the total electronic density contour plots. In general, total electronic density contour plots tend to exhibit higher values at and close to atomic centers and lower values within the surroundings of chemical bonds. Consequently, these plots do not depict chemical bonds as clearly as $\sigma_{iso}(\mathbf{r})$ contour plots.

The behavior of the isotropic shielding above (and below) the molecular planes of furan, pyrrole, and thiophene is illustrated by the $\sigma_{iso}(\mathbf{r})$ contour plots in planes 0.5 and 1 Å above the respective molecular planes shown in Figures 4−6. The height of 1 Å above the molecular plane corresponds to a popular NICS index, NICS(1),[9,10] while 0.5 Å is close to the height of 1 Bohr above the molecular plane at which the current is usually displayed in ring current maps (see e.g., ref 12). Cordell and Boggs reported HF-level total electronic density contour plots for furan, pyrrole, and thiophene in planes 0.2 and 0.8 Å above the respective molecular planes and concluded that, while the 0.2 Å plots still exhibited significant σ character, the 0.8 Å plots were dominated by π contributions.[23] In the opinion of these authors, the most uniform delocalization of the total electron density was observed in pyrrole, followed by thiophene and furan. As this implies an ordering of aromaticities identical to the one following from the NICS(0) values calculated by Schleyer and et al.,[7] it is likely that the use of insufficiently large basis sets can affect, in very much the same manner, predictions based on different aromaticity criteria.

In the $\sigma_{iso}(\mathbf{r})$ contour plots at 0.5 Å above the molecular planes (see Figures 4a−6a), we can still see some σ character associated with the protrusions over carbon−hydrogen (and, in pyrrole, nitrogen−hydrogen) bonds. At a height of 1 Å above the molecular plane these protrusions all but disappear (see Figures 4b−6b), and we are left with very simple pictures which clearly show that $\sigma_{iso}(\mathbf{r})$ is most uniformly delocalized in thiophene, followed by pyrrole and furan.

Kleinpeter et al. have reported ICSSs corresponding to selected values of the "through space NMR shieldings," that is, of $\sigma_{iso}(\mathbf{r})$, for a number of aromatic and antiaromatic molecules including furan, pyrrole, and thiophene.[14] Looking at the extents of the ICSSs corresponding to $\sigma_{iso}(\mathbf{r})$ = 0.1, these authors concluded that thiophene was "chemically nearest" to benzene. However, because of the use of a coarser grid with a spacing of 0.5 Å, which is 10 times larger than the one used in the current work, most of the finer, but very important, details of the $\sigma_{iso}(\mathbf{r})$ behavior in the vicinity of nuclei and over chemical bonds are missing from the plots shown in reference 14 and have not been observed and discussed previously.

dx.doi.org/10.1021/jo401319k | J. Org. Chem. 2013, 78, 8037−8043

4. CONCLUSIONS

The detailed study of the changes in the isotropic shielding $\sigma_{iso}(\mathbf{r})$ within the regions of space surrounding the five-membered heterocycles furan, pyrrole, and thiophene highlights important features of the chemical bonding in these systems and provides a convenient way of comparing their relative aromaticities.

The $\sigma_{iso}(\mathbf{r})$ contour plots in the molecular planes of furan, pyrrole, and thiophene clearly suggest that while the carbon−carbon double bonds in each of these molecules are stronger than the carbon−carbon single bond, the difference is not very pronounced, which is also supported by the fact that the highest $\sigma_{iso}(\mathbf{r})$ values over double and single bonds vary by just ca. 2−5 ppm (see Table 2).

Established experimental evidence about the reactivities of furan, pyrrole, and thiophene indicates that aromaticity decreases in the order thiophene > pyrrole > furan. Most qualitative and quantitative measures of aromaticity confirm this order (for a detailed overview, see ref 21). While previous NICS(0) calculations at the HF-GIAO/6-31+G* and HF-GIAO/6-31G* levels of theory[7] endorsed a different classification, pyrrole > thiophene > furan, our HF-GIAO/6-311++G(d,p) and MP2-GIAO/6-311++G(d,p) NICS(0), NICS(0.5), and NICS(1) results support the widely accepted order thiophene > pyrrole > furan (see Table 1). The relatively small differences between our HF-GIAO and MP2-GIAO NICS values suggest that accurate NICS calculations on aromatic systems benefit more from the use of an extended basis set than from the inclusion of dynamical electron correlation effects.

A previous study of the variations of the isotropic shielding in and around two well-known examples of aromatic and antiaromatic systems, benzene and square cyclobutadiene, has shown that $\sigma_{iso}(\mathbf{r})$ is completely delocalized around the benzene ring, forming a doughnut-shaped region of increased shielding surrounding the carbon−carbon bonds, whereas in square cyclobutadiene the presence of a large deshielded dumbbell-shaped central region disrupts the connections between the shielded regions outlining individual carbon−carbon bonds, decreases the shielding within these regions, and displaces them to off-bond locations outside the ring.[15] The analysis of the behavior of $\sigma_{iso}(\mathbf{r})$ in and around furan, pyrrole, and thiophene confirms the connection between aromaticity and isotropic shielding delocalization. The different extents of $\sigma_{iso}(\mathbf{r})$ delocalization observed in these five-membered rings, as well as a number of more subtle features of $\sigma_{iso}(\mathbf{r})$, are consistent with a reduction in aromaticity in the order thiophene > pyrrole > furan. Our results indicate that the isotropic shielding delocalization is most obvious in $\sigma_{iso}(\mathbf{r})$ contour plots in planes 1 Å above the respective molecular planes (see Figures 4b−6b), which are dominated by the π contributions to $\sigma_{iso}(\mathbf{r})$. It is expected that $\sigma_{iso}(\mathbf{r})$ contour plots of this type will prove very useful while comparing the relative aromaticities of a much wider range of aromatic systems.

Clearly, analyzing the behavior of $\sigma_{iso}(\mathbf{r})$ within the region of space surrounding a molecule is significantly more time-consuming than the evaluation of single-value aromaticity indices such as NICS, magnetic susceptibility exaltations, aromatic stabilization energies, etc. However, as demonstrated by the results we have obtained so far, the detailed picture of the way in which aromaticity or antiaromaticity modifies the shielding distribution, produced by an analysis of this type, justifies the effort and supports the argument that aromaticity is a multidimensional characteristic which cannot be fully described by a single numerical criterion.[24]

AUTHOR INFORMATION

Corresponding Author

*E-mail: peter.karadakov@york.ac.uk.

Notes

The authors declare no competing financial interest.

ACKNOWLEDGMENTS

The authors thank the Department of Chemistry of the University of York for a Teaching Scholarship to K.E.H.

REFERENCES

(1) Johnson, C. E.; Bovey, F. A. *J. Chem. Phys.* **1958**, *29*, 1012−1014.
(2) Wannere, C. S.; Schleyer, P. v. R. *Org. Lett.* **2003**, *5*, 605−608.
(3) Martin, N. H.; Loveless, D. M.; Main, K. L.; Wade, D. C. *J. Mol. Graphics Modell.* **2006**, *25*, 389−395.
(4) Martin, N. H.; Rowe, J. E.; Pittman, E. L. *J. Mol. Graphics Modell.* **2009**, *27*, 853−859.
(5) Martin, N. H.; Teague, M. R.; Mills, K. H. *Symmetry* **2010**, *2*, 418−436.
(6) Martin, N. H.; Brown, J. D.; Nance, K. H.; Schaefer, H. F.; Schleyer, P. v. R.; Wang, Z. X.; Woodcock, H. L. *Org. Lett.* **2001**, *3*, 3823−3826.
(7) Schleyer, P. v. R.; Maerker, C.; Dransfeld, A.; Jiao, H.; Hommes, N. J. R. v. E. *J. Am. Chem. Soc.* **1996**, *118*, 6317−6318.
(8) Schleyer, P. v. R.; Jiao, H.; Hommes, N. J. R. v. E.; Malkin, V. G.; Malkina, O. L. *J. Am. Chem. Soc.* **1997**, *119*, 12669−12670.
(9) Schleyer, P. v. R.; Manoharan, M.; Wang, Z. X.; Kiran, B.; Jiao, H.; Puchta, R.; Hommes, N. J. R. v. E. *Org. Lett.* **2001**, *3*, 2465−2468.
(10) Fallah-Bagher-Shaidaei, H.; Wannere, C. S.; Corminboeuf, C.; Puchta, R.; Schleyer, P. v. R. *Org. Lett.* **2006**, *8*, 863−866.
(11) Lazzeretti, P. *Phys. Chem. Chem. Phys.* **2004**, *6*, 217−223.
(12) Fias, S.; Fowler, P. W.; Delgado, J. L.; Hahn, U.; Bultinck, P. *Chem.—Eur. J.* **2008**, *14*, 3093−3099.
(13) Klod, S.; Kleinpeter, E. *J. Chem. Soc., Perkin Trans. 2* **1989**, 1893−1898.
(14) Kleinpeter, E.; Klod, S.; Koch, A. *J. Mol. Struct.: THEOCHEM* **2007**, *811*, 45−60.
(15) Karadakov, P. B.; Horner, K. E. *J. Phys. Chem. A* **2013**, *117*, 518−523.
(16) Mata, F.; Martin, M. C.; Sørensen, G. O. *J. Mol. Struct.* **1978**, *48*, 157−163.
(17) Nygaard, L.; Nielsen, J. T.; Kirchheiner, J.; Maltesen, G.; Rastrup-Andersen, J.; Sørensen, G. O. *J. Mol. Struct.* **1969**, *3*, 491−506.
(18) Bak, B.; Christensen, D.; Hansen-Nygaard, L.; Rastrup-Andersen, J. *J. Mol. Spectrosc.* **1961**, *7*, 58−63.
(19) Frisch, M. J.; Trucks, G. W.; Schlegel, H. B.; Scuseria, G. E.; Robb, M. A.; Cheeseman, J. R.; Scalmani, G.; Barone, V.; Mennucci, B.; Petersson, G. A. et al. *Gaussian 09*, Revision B.01; Gaussian, Inc.: Wallingford CT, 2009.
(20) Schleyer, P. v. R.; Jiao, H. *Pure Appl. Chem.* **1996**, *68*, 209−218.
(21) Katritzky, A. R.; Ramsden, C. A.; Joule, J.; Zhdankin, V. V. *Handbook of Heterocyclic Chemistry*, 3rd ed.; Elsevier: Amsterdam, 2010, ISBN-10: 0080958435, ISBN-13: 978-0080958439, pp 126−128.
(22) Chen, Z.; Wannere, C. S.; Corminboeuf, C.; Puchta, R.; Schleyer, P. v. R. *Chem. Rev.* **2005**, *105*, 3842−3888.
(23) Cordell, F. R.; Boggs, J. E. *J. Mol. Struct.: THEOCHEM* **1981**, *85*, 163−178.
(24) Katritzky, A. R; Karelson, M.; Sild, S.; Krygowski, T. M.; Jug, K. *J. Org. Chem.* **1998**, *63*, 5228−5231.